J Neurooncol
DOI 10.1007/s11060-013-1082-x

LABORATORY INVESTIGATION

Murine cell line model of proneural glioma for evaluation of anti-tumor therapies

Adam M. Sonabend · Jonathan Yun · Liang Lei · Richard Leung · Craig Soderquist · Celina Crisman · Brian J. Gill · Arthur Carminucci · Julia Sisti · Mike Castelli · Peter A. Sims · Jeffrey N. Bruce · Peter Canoll

Received: 24 October 2012 / Accepted: 13 February 2013

Abstract Molecular subtypes of glioblastoma (GBM) with distinct alterations have been identified. There is need for reproducible, versatile preclinical models that resemble specific GBM phenotypes to facilitate preclinical testing of novel therapies. We present a cell line-based murine proneural GBM model and characterize its response to radiation therapy. Proneural gliomas were generated by injecting PDGF-IRES-Cre retrovirus into the subcortical white matter of adult mice that harbor floxed tumor suppressors (Pten and p53) and stop-floxed reporters. Primary cell cultures were generated from the retrovirus induced tumors and maintained in vitro for multiple passages. RNA sequencing-based expression profiling of the resulting cell lines was performed. The tumorigenic potential of the cells was assessed by intracranial injection into adult naïve mice from different strains. Tumor growth was assessed by bioluminescence imaging (BLI). BLI for tumor cells and brain slices were obtained and compared to in vivo BLI. Response to whole-brain radiation was assessed in glioma-bearing animals. Intracranial injection of $Pdgf^{+}Pten^{-/-}p53^{-/-}luciferase^{+}$ glioma cells led to formation of GBM-like tumors with 100 % efficiency ($n = 48$) and tumorigenesis was retained for more than 3 generations. The cell lines specifically resembled proneural GBM based on expression profiling by RNA-Seq. $Pdgf^{+}Pten^{-/-}p53^{-/-}luciferase^{+}$ cell number correlated with BLI signal. Serial BLI measured tumor growth and correlated with size and location by ex vivo imaging. Moreover, BLI predicted tumor-related mortality with a 93 % risk of death within 5 days following a BLI signal between 1×10^8 and 5×10^8 photons/s cm^2. BLI signal had transient but significant response following radiotherapy, which corresponded to a modest survival benefit for radiated mice ($p < 0.05$). Intracranial injection of $Pdgf^{+}Pten^{-/-}p53^{-/-}luciferase^{+}$ cells constitutes a novel and highly reproducible model, recapitulating key features of human proneural GBM, and can be used to evaluate tumor-growth and response to therapy.

Keywords Glioma · Proneural · Murine · Radiotherapy · Cell line

Electronic supplementary material The online version of this article (doi:10.1007/s11060-013-1082-x) contains supplementary material, which is available to authorized users.

A. M. Sonabend · J. Yun · C. Soderquist · C. Crisman · B. J. Gill · A. Carminucci · J. N. Bruce
Gabriele Bartoli Brain Tumor Laboratory, Department of Neurosurgery, Columbia University Medical Center, 1130 St. Nicholas Ave Rm. 1001, New York, NY 10032, USA

L. Lei · R. Leung · J. Sisti · M. Castelli · P. Canoll (✉)
Department of Pathology and Cell Biology, Columbia University Medical Center, Herbert Irving Cancer Research Center, 1130 St. Nicholas Ave Rm. 1001, New York, NY 10032, USA
e-mail: pc561@columbia.edu

P. A. Sims
Department of Biochemistry & Molecular Biophysics, Columbia University Medical Center, 1130 St. Nicholas Ave Rm. 1001, New York, NY 10032, USA

P. A. Sims
The Columbia Initiative in Systems Biology, Columbia University Medical Center, 1130 St. Nicholas Ave Rm. 1001, New York, NY 10032, USA

Introduction

A great deal of the research in glioblastoma (GBM) relies on cell lines artificially selected to grow in vitro, which presents issues for use as tumor models. First, the genetic profile of passaged cell lines does not fully reflect that seen in human gliomas [1, 2]. Also, many of these cell lines give

Published online: 16 March 2013

rise to tumors that do not resemble human gliomas histologically [3]. Consequently, pre-clinical results often do not translate accurately to clinical trials and practice. The search for better glioma models is necessary for advancing the field of neurooncology. Moreover, a pre-clinical, cell line-based model that allows for in vitro as well as in vivo studies would allow for efficient and comprehensive testing of experimental therapies.

Glioblastoma has been classified into four categories based on expression-based profiling: proneural, neural, mesenchymal and classical [4]. Proneural GBM, which includes most of secondary GBM and a distinct subset of primary GBM, is characterized by p53, IDH1/2 mutations and PDGFR amplifications [4–6]. Recently, our group generated a transgenic mouse glioma model with a proneural phenotype by transforming white matter glial progenitors in vivo. Genome-wide expression analyses and cross-species comparisons with the TCGA data revealed that the mouse tumors most resembled the proneural subtype of GBM and that both mouse and human proneural gliomas were significantly enriched for genes expressed by oligodendrocyte progenitor cells (OPC) [7]. Here, we show that cells isolated from these tumors can be cultured for multiple passages while retaining their proneural phenotype and their capacity to generate tumors that recapitulate GBM. These mouse glioma cells express luciferase and therefore, tumor growth and response to therapy can be followed by luciferase-based bioluminescence imaging (BLI). We describe the effects achieved by radiotherapy, a standard of care for human GBM. This model is a versatile tool to evaluate novel adjuvant therapies for proneural GBM.

Methods

Retrovirus production and injections

A 0.8 kb fragment encoding PDGF-B-hemagglutinin (HA) [8] was ligated into the MCS1 region and Cre was ligated into the MCS2 region of the retroviral vectors pQCXIX. Using these constructs, replication-deficient viruses with vsv-G coats were generated as previously described [9]. Viral titers were established in colony-forming units (CFU) by incubating YFP$^{-stop\text{-}lox}$ mouse embryonic fibroblasts with serial dilutions of retrovirus in tenfold steps. At 48 h, the number YFP cell clusters were counted. This number was multiplied by the dilution factor in order to determine the CFU. Virus was then injected into the subcortical white matter (stereotactic coordinates relative to bregma: 2.1 mm lateral, 2.1 mm rostral, 1.8 mm deep) of adult Pten$^{ox/lox}$/p53$^{lox/lox}$/luciferase-$^{stop\text{-}lox}$ transgenic mice using a Hamilton syringe with a 33 gauge needle (0.4 µl at 0.2 µl/min) [7]. These mice have been backcrossed B6(Cg)-*Tyr*$^{c-2J}$/J, or B6-albino mice, for more than 10 generations, resulting in white mice that are suitable for BLI.

Tumor cell isolation and injection

All mice developed tumors with retrovirus injection. Following IACUC guidelines, animals were sacrificed at the first sign of morbidity. Ex-vivo gross total resection of the tumor was performed and tumor cells were isolated using enzymatic digestion [10, 11]. The isolated cells were cultured for up to 15 passages in a 2:1 ratio of basal media (DMEM, N2, T3, 0.5 % FBS, and penicillin/streptomycin/amphotericin) in B104 conditioned media [5]. This media was further supplemented with PDGF-AA (Sigma-Aldrich; St. Louis, MO) and FGFb (Gibco; Grand Island, NY, USA) to a concentration of 10 ng/ml. Intracranial injection of the freshly prepared tumor cells was performed as previously described for the retrovirus. 1.0×10^4, 2.0×10^4, and 1.0×10^5 cells were injected into 3 naïve adult Pten$^{lox/lox}$/p53$^{lox/lox}$/luciferase-$^{stop\text{-}lox}$ transgenic mice over 3 generations.

Survival study

Two separate cohorts of mice harboring floxed p53 and Pten and stop-floxed luciferase were injected with 2.0×10^4 Pdgf^{+}Pten$^{-/-}$p53$^{-/-}$ tumor cells isolated from two different primary tumors (Cohort 1 $n = 12$, Cohort 2 $n = 6$) and were observed daily and sacrificed at first signs of morbidity, including weight loss, seizures, and hemorrhage. A parallel study was performed in FvB backround mice injected with 2.0×10^4 Pdgf^{+}Pten$^{-/-}$p53$^{-/-}$ tumor cells. Brains were either fixed in 4 % paraformaldehyde and examined histologically or were prepared for culture and transplant into naïve mice using the conditions previously described.

Bioluminescence imaging of cellular suspensions of digested tumors

Tumor cells were plated at different cell densities in a 24-well plate; 3.0×10^3, 3.0×10^4, and 3.0×10^5 cells per well, each in triplicate. 300 µl of a 0.30 mg/ml solution of D-Luciferin (Fisher Scientific, Waltham, MA) was added to each well and luminescence was measured using the Xenogen IVIS 200 using Living Image 3.2 (Xenogen; Hopkinton, MA, USA) after 10 min.

Bioluminescence imaging of in vivo tumor burden

Mice injected with tumor cells were anesthetized with 2.5 % isofluorane and injected intraperitoneally with 3 mg of D-Luciferin. BLI was performed 10 min after injection

with a region of interest (2.25 cm) centered upon the mouse's head.

Bioluminescence imaging of ex vivo brain slices

Mice to undergo the ex vivo imaging were euthanized following the final in vivo image acquisition. The brain was removed and sectioned into 1.0 mm thick slices. Each slice was placed in a 1 cm well containing PBS. 300 µl of a 0.30 mg/ml solution of D-luciferin was added to each well and incubated for 10 min before BLI was measured. The sum BLI of the slices represented the ex vivo total. This was compared to the in vitro and in vivo BLI using linear regression (Microsoft Excel).

In vivo radiation treatment

Mice were imaged on the 6th day following injection of 2.0×10^4 tumor cells and randomly assigned to treatment groups ($n = 24$). Radiation was delivered with a Mark 1 Cesium-137 irradiator (JL Shepherd and Associates; San Fernando, CA) at 6 Gy per day for 10 days. Each individual mouse placed behind a 1.4 cm lead barrier designed to target the head. Treatment took place on 6–10 dpi and 13–17 dpi, with holidays on days 11 and 12.

Immunohistochemistry and microscopy

Brains for immunohistochemistry were fixed by cardiac perfusion with 4 % paraformaldehyde. Hematoxylin and eosin stains and immunoperoxidase stains were performed using the following antibodies: anti-Olig2 (1:500; Chemicon; Temecula, CA, USA), anti-GFAP (1:1000; Chemicon; Temecula, CA), anti-Ki67 (1:1000, Vector, Burlingame, CA), and anti-PDGFR$_\alpha$ (1:500; Cell Signaling, Beverly, MA, USA). Stained sections were examined and photographed using a fluorescent microscope (Zeiss; Oberkochen, Germany) and analyzed with Metamorph (Molecular Devices; Sunnyvale, CA, USA).

RNA-Seq based classification of tumor cell line and identification of proneural subtype

We measured genome-wide expression profiles of three mouse tumor cell lines and four virus-induced mouse tumors by RNA-Seq. For each sample, we obtained 15–30 million single-end, 100-base reads on an Illumina HiSeq 2000 sequencer. We rank-ordered the expression levels of the GBM subtype classifier genes obtained from RNA sequencing of our tumor and cell line samples. We then rank-ordered the expression levels of these same genes in the 202 TCGA human microarray data sets for which GBM subtype information is available [4]. For each tumor and cell line RNA-Seq data set, we calculated the Spearman's rank correlation coefficient with each subtyped human microarray data set. This provides an estimate of statistical dependence between the mouse tumor and cell line expression profiles and those of human samples from each of the four GBM subtypes without assumptions about the functional relationship between microarray expression levels and those obtained by RNA-Seq. We use the median value of the correlation between an RNA-Seq data set and the TCGA microarray data for a given subtype as a similarity score for that subtype.

To validate this approach, we used the same correlation calculation to classify the small number of available subtyped TCGA samples that have corresponding RNA-Seq data sets. Our method correctly classified 7/8 proneural samples, 8/10 Mesenchymal samples, and 5/5 Classical samples. In cases where the incorrect subtype was identified, the correct subtype was consistently the second most similar subtype. However, the neural subtype was more ambiguous, and only 2/7 Neural samples were called correctly.

Results

Pdgf$^+$Pten$^{-/-}$p53$^{-/-}$luciferase$^+$ cells form murine glioblastomas and resemble the proneural phenotype

Injection of Pdgf$^+$Pten$^{-/-}$p53$^{-/-}$luciferase$^+$ glioma cells led to formation of GBM-like tumors with 100 % efficiency for tumor cells passaged for up to 15 generations. Furthermore, these cells retained tumor-forming capacity over at least three generations of serial intracranial transplantation. This is similar to what was seen following intracranial injection of freshly isolated cells into NOD/SCID mice [7]. Comparison of the subtype-specific genes based on level of expression of the mouse cell line ($n = 3$) and virus-induced tumors ($n = 4$) by RNA-Seq to ordered classifier gene sets in the TCGA yielded the strongest correlation with the proneural subtype (Fig. 1) [4] (source data available download at GEO at http://www.ncbi.nlm.nih.gov/geo/; Reference number: GSE45031). This observation is summarized (Table 1), which shows the median Spearman's rank correlation coefficients between expression profiles of the four mouse tumors or three mouse cell lines and the subtyped human GBM expression profiles from the TCGA (http://cancergenome.nih.gov/) ($n = 202$).

The tumors recapitulated histological features of human GBM, including glomeruloid vascular proliferation, pseudopalisading necrosis, and diffusely infiltrative edges (Fig. 2a). Immunohistochemical stains showed the majority of tumor cells strongly positive for Pdgfr alpha and Olig-2, while Gfap staining was seen predominantly in

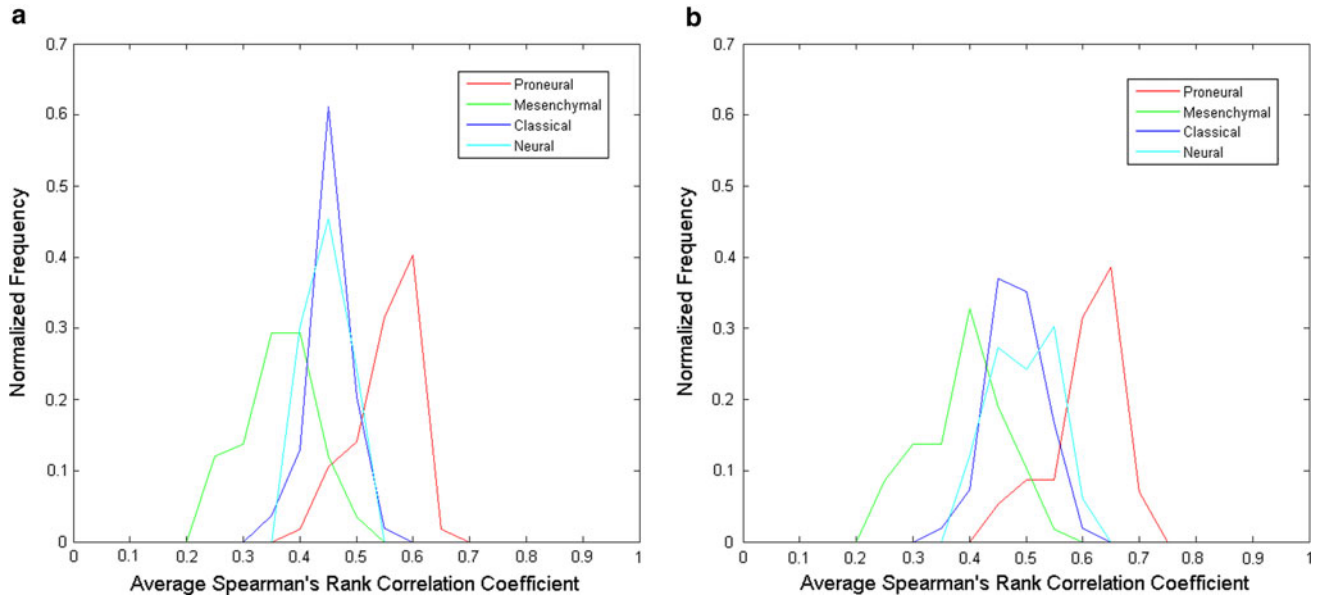

Fig. 1 Histograms showing the Spearman's rank correlation coefficients between human GBM expression profiles from the TCGA for samples representing each of the four GBM subtypes in the TCGA data (proneural $n = 57$, neural $n = 33$, classical $n = 54$, mesenchymal $n = 58$) and **a** mouse tumor (averaged over four samples) and **b** mouse cell line (averaged over three samples) RNA-Seq profiles. Both the mouse tumors and cell lines, are most similar to the proneural subtype of human GBM

Table 1 Spearman correlations between either $Pdgf^{+}Pten^{-/-}p53^{-/-}$ cell lines or virus-induced tumors, and the four different subtypes of human GBM from the TCGA dataset according to the Verhaak et al. [4] classifications

	Proneural	Mesenchymal	Classical	Neural
Mouse tumor 1	0.62	0.39	0.49	0.48
Mouse tumor 2	0.61	0.38	0.47	0.50
Mouse tumor 3	0.62	0.39	0.48	0.51
Mouse tumor 4	0.64	0.40	0.50	0.50
Mouse cell line 1	0.57	0.37	0.45	0.45
Mouse cell line 2	0.54	0.35	0.43	0.43
Mouse cell line 3	0.57	0.38	0.46	0.47

astrocytes distributed throughout the tumor (Fig. 2b–d), These results are consistent with the pattern of staining seen in the initial, virus induced tumors [7].

Bioluminescence correlates with glioma size and localization and predicts onset of tumor-related morbidity

Luciferase expression enabled the reporting of growth dynamics and response to treatments in our cell lines and corresponding brain tumors. In vitro, luminescence correlated with number of $Pdgf^{+}Pten^{-/-}p53^{-/-}luciferase^{++}$ glioma cells (Fig. 3a). Next, we compared the in vivo luminescence of these tumors with the sum, ex vivo luminescence of brain serially sectioned. On average, the in vivo luminescence was 4.4 times lower than the sum luminescence of the slices, presumably from the quenching of signal by overlying tissue. Nevertheless, there was a direct correlation between in vivo and ex vivo luminescence, observed in small and large tumors (Fig. 3b). Moreover, luminescence distribution co-localized with the anatomic locations of the tumors (Fig. 3c). Thus, in vivo luminescence quantitatively follows tumor size and growth dynamics. Furthermore, luminescence was predictive of morbidity and mortality. 93 % morbidity was seen during a 5-day period following a luminescence measurement between 1×10^8 and 5×10^8 photons/s cm^2 (Fig. 4).

Cell-based $Pdgf^{+}Pten^{-/-}p53^{-/-}luciferase^{+}$ gliomas show reproducible growth dynamics and are susceptible to radiotherapy

Two separate cell lines isolated from different primary tumors underwent 6 passages and then assessed in vivo following intracranial injection. BLI, as a surrogate for growth dynamics and tumor burden, and survival (27 vs. 29 days, log rank $p = 0.35$) were indistinguishable between the two cohorts (Supplementary Figure).

To evaluate whether $Pdgf^{+}Pten^{-/-}p53^{-/-}$ cells can engraft in different strains, a similar experiment with equal number of cells (2×10^4 cells) was performed on mice from FvB strain ($n = 7$). There was 100 % tumor penetrance. Whereas there were no significant differences in tumor growth kinetics, as measured by BLI, a modest but significant increase in survival was noticed for the FvB group compared to survival data when cells were injected

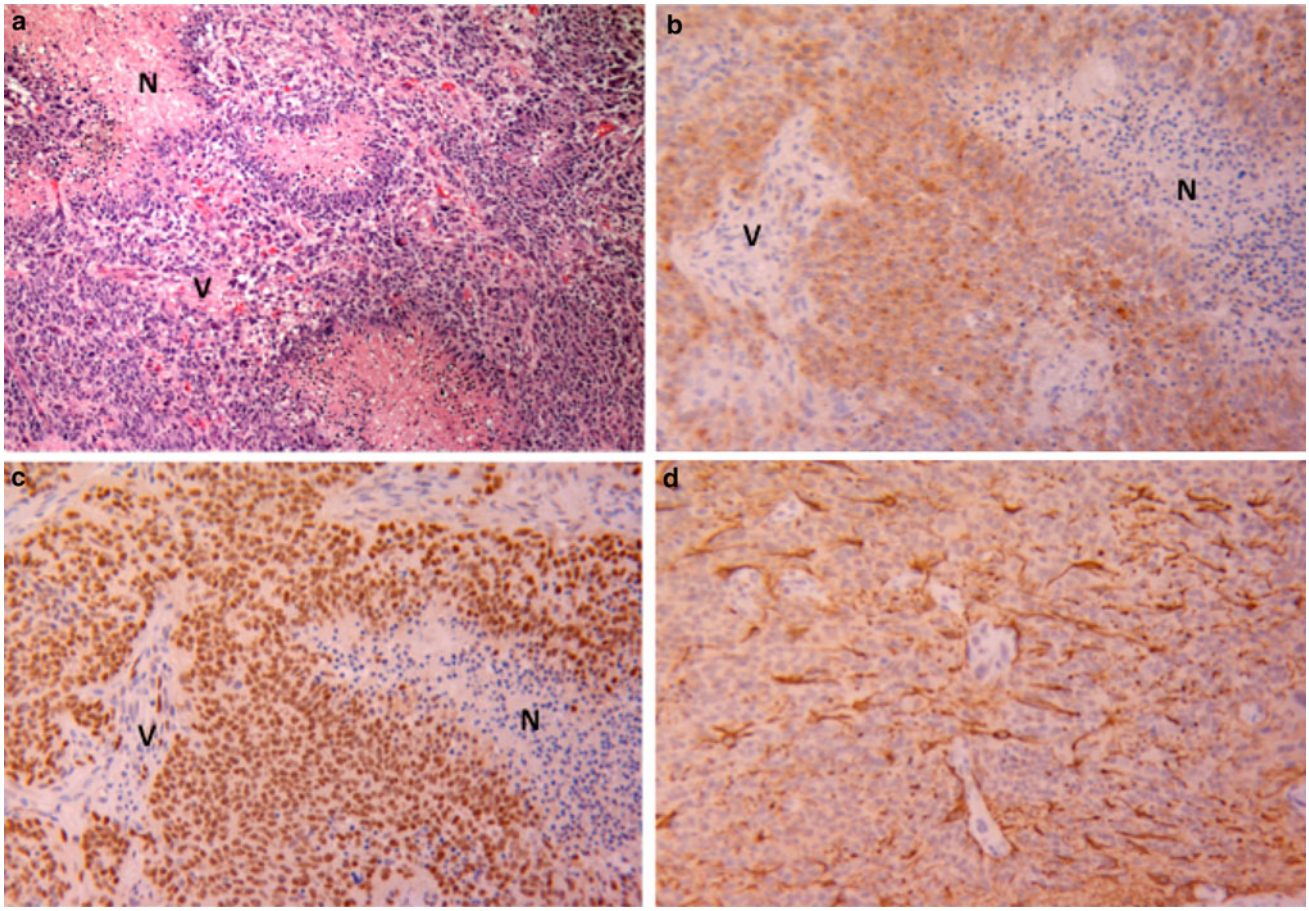

Fig. 2 Injection of Pdgf^{+}Pten$^{-/-}$p53$^{-/-}$luciferase^{+} cells form GBM-like tumors stained for **a** H&E, **b** IHC for Pdgfra, **c** Olig 2, and **d** Gfap. Necrosis (N) and vascular proliferation (V) and Cortex (CX) are delineated

into Pten$^{lox/lox}$/p53$^{lox/lox}$/luciferase-$^{stop\text{-}lox}$ mice that are syngeneic to the cell line (cohorts 1 and 2) (log rank $p < 0.05$) (Supplementary Figure).

Response to radiation demonstrates utility of this model for assessing therapies. BLI was decreased for radiated versus control mice at 22 and 24 dpi ($p < 0.05$) (Fig. 5a). Though this difference was lost over time, a modest but significant increase in survival was noted (33 days in treated vs. 27 days in controls, $p = 0.0055$) (Fig. 5b). These findings are similar to our previous work using cells that were freshly isolated from the retrovirus induced tumors [12], demonstrating the therapeutic responsiveness of these cell lines remains consistent over multiple passages and across separate tumor preparations.

Discussion

Distinguishing promising cancer treatments that merit clinical testing and defining the molecular characteristics of the patients that will benefit from these treatments are formidable challenges. Overcoming this issue is key for development of effective therapies for GBM, for which distinct molecular subgroups exist [4]. We present a mouse model of proneural GBM that consists on Pdgf^{+}Pten$^{-/-}$p53$^{-/-}$luciferase^{+} glioma cells. We characterize this cell-based model, and show its features as a convenient and relevant model for pre-clinical testing. To illustrate its utility, we tested the response to radiation therapy, a major component of the standard of care for this disease.

This cell-based model combines the advantages of the genetically engineered and retrovirus-based tumor models. Tumors are generated with well-defined genetic alterations (Pdgf pathway activation, p53 and Pten loss of function) commonly seen on human GBM. Moreover, this model offers the possibility of genetic manipulation and experimentation in vitro as well as in vivo. Furthermore, this model accurately recapitulates the histopathologic hallmarks of GBM including pseudopalisading necrosis, diffuse infiltration, and vascular proliferation. These histological characteristics contrast sharply with human xenografts from traditional established cell lines still in use [13–15], which tend to grow as dense clusters of tumor cells with little invasion. Alternative cell-based glioma

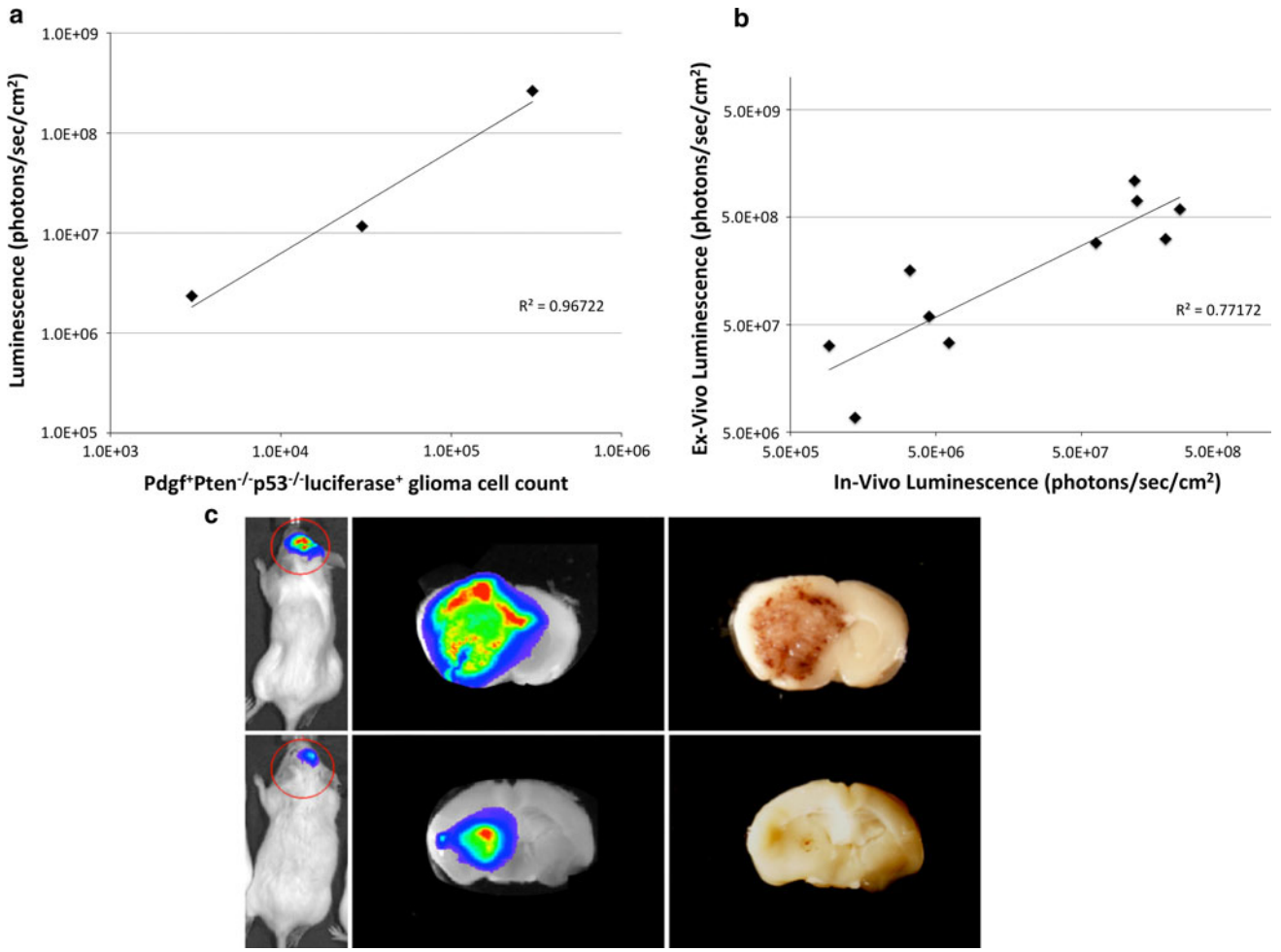

Fig. 3 **a** Strong correlation between BLI signal and in vitro cell number is observed. **b** The in vivo BLI signal correlates with the sum total signal acquired from acute *ex vivo* brain slices of the same tumors. **c** The distribution of luminescence co-localizes with the anatomic location of the tumor

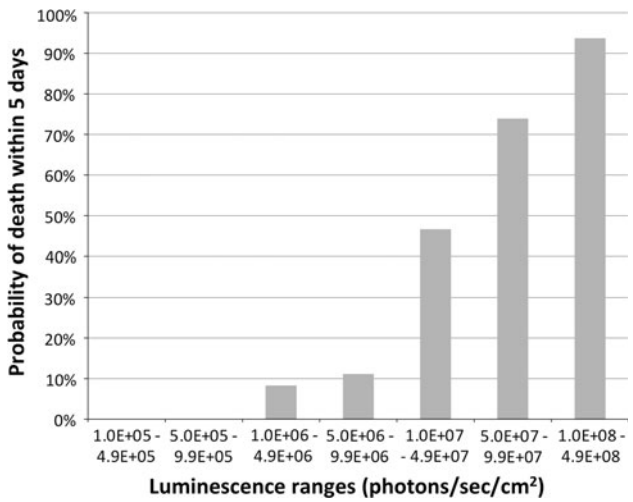

Fig. 4 Luminescence is predictive of mortality, with bioluminescence between 1.0×10^8 and 5.0×10^8 photons/s cm^2 being associated with a 93 % risk of death in 5 days

models with a more realistic histological profile are available, but are usually based on human glioma cell preparations requiring immunocompromised rodent hosts for in vivo experiments [15]. This issue might potentially give rise to artificial cross species microenvironment interactions between host and tumor cells, and limit the study of tumor immunology. An alternative to the cell line models include retrovirus/transgenic mouse gliomas systems [7, 8], which are powerful models, but involve transgenic mouse and virus-related resources that may not be available to some researchers. The use of cell lines generated from retrovirus/transgenic mouse models provides a convenient and accessible alternative, and offer the possibility of in vitro analyses to compliment the in vivo studies.

Another strength of this cell-based system is the ability for non-invasive quantification of tumor growth by BLI, which may represent a more sensitive indicator of response to therapy than overall survival. Furthermore, serial

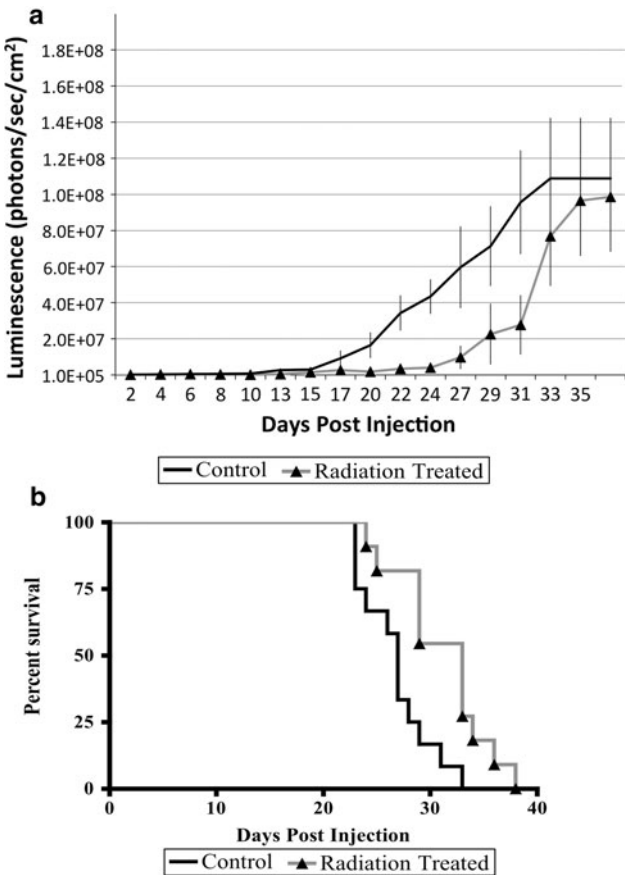

Fig. 5 **a** Tumor growth by luminescence, is slowed by administration of fractionated radiation (total 60 Gy, 6 Gy/day for 10 days), most significant between 22 and 24 dpi. **b** This translates to a modest, but significant, survival benefit (33 days for treated vs. 27 days for control)

luciferase imaging allows for longitudinal monitoring of tumor growth dynamics in the setting of therapies and may be useful for evaluating treatments and their combinations. Using this approach, wide ranges of anti-tumor therapies can be screened in vitro using this cell line before pursuing more costly in vivo experiments, either in retrovirus or cell line-based tumors.

In this study, we have demonstrated that $Pdgf^{+}Pten^{-/-}p53^{-/-}$ cell lines specifically resemble the gene expression profile of human proneural GBM. The cell lines analyzed were expanded over 6 passages in culture and retained the proneural phenotype. Silber et al. [16] and Schulte et al. [17] have recently reported human glioma cell lines that retain a proneural expression profile while grown in vitro in serum free media. Our cell-based model is a good complement to these lines as given its murine origin, it allows their implantation into immunocompetent hosts.

We present a murine proneural GBM model with genetic and histological resemblance to human proneural GBM and show a modest response to radiation therapy. For these reasons, we offer this convenient glioma cell line model to the neurooncology research community as a tool to evaluate novel treatments for this devastating disease. In future studies, it will be important to identify the genetic and epigenetic alterations that accumulate in this model, and characterize how they relate to alterations that occur in the different types of human proneural gliomas [18, 19].

Acknowledgments Funding provided by the NIH/NINDS grant 1R01NS066955 (P.C). P.A.S. is supported by the NIH/NIBIB grant 1K01EB016071. We thank TCGA for making expression data on human gliomas available for this work. We thank JP Sulzberger *Columbia Genome Center* for RNA sequencing of the mouse tumors and cell lines.

Conflict of interest The authors declare that there are no conflicts of interest.

Ethical standards All experiments were conducted in compliance with institutional IACUC protocols.

References

1. Gerlach B, Harder AH, Hulsebos TJ, Leenstra S, Slotman BJ, Vandertop WP, Hartmann KA, Sminia P (2002) Radiosensitivity and TP 53, EGFR amplification and LOH10 analysis of primary glioma cell cultures. Strahlenther Onkol 178:491–496
2. Thomas C, Ely G, James CD, Jenkins R, Kastan M, Jedlicka A, Burger P, Wharen R (2001) Glioblastoma-related gene mutations and over-expression of functional epidermal growth factor receptors in SKMG-3 glioma cells. Acta Neuropathol 101: 605–615
3. Finkelstein SD, Black P, Nowak TP, Hand CM, Christensen S, Finch PW (1994) Histological characteristics and expression of acidic and basic fibroblast growth factor genes in intracerebral xenogeneic transplants of human glioma cells. Neurosurgery 34: 136–143
4. Verhaak RG, Hoadley KA, Purdom E, Wang V, Qi Y, Wilkerson MD, Miller CR, Ding L, Golub T, Mesirov JP, Alexe G, Lawrence M, O'Kelly M, Tamayo P, Weir BA, Gabriel S, Winckler W, Gupta S, Jakkula L, Feiler HS, Hodgson JG, James CD, Sarkaria JN, Brennan C, Kahn A, Spellman PT, Wilson RK, Speed TP, Gray JW, Meyerson M, Getz G, Perou CM, Hayes DN (2010) Integrated genomic analysis identifies clinically relevant subtypes of glioblastoma characterized by abnormalities in PDGFRA, IDH1, EGFR, and NF1. Cancer Cell 17:98–110. doi: 10.1016/j.ccr.2009.12.020
5. Canoll PD, Musacchio JM, Hardy R, Reynolds R, Marchionni MA, Salzer JL (1996) GGF/neuregulin is a neuronal signal that promotes the proliferation and survival and inhibits the differentiation of oligodendrocyte progenitors. Neuron 17:229–243. doi:S0896-6273(00)80155-5
6. Phillips HS, Kharbanda S, Chen R, Forrest WF, Soriano RH, Wu TD, Misra A, Nigro JM, Colman H, Soroceanu L, Williams PM, Modrusan Z, Feuerstein BG, Aldape K (2006) Molecular subclasses of high-grade glioma predict prognosis, delineate a pattern of disease progression, and resemble stages in neurogenesis. Cancer Cell 9:157–173. doi:1016/j.ccr.2006.02.019
7. Lei L, Sonabend AM, Guarnieri P, Soderquist C, Ludwig T, Rosenfeld S, Bruce JN, Canoll P (2011) Glioblastoma models

reveal the connection between adult glial progenitors and the proneural phenotype. PLoS One 6(5):e20041. doi:10.1371/journal.pone.0020041
8. Shih AH, Dai C, Hu X, Rosenblum MK, Koutcher JA, Holland EC (2004) Dose-dependent effects of platelet-derived growth factor-B on glial tumorigenesis. Cancer Res 64:4783–4789. doi:10.1158/0008-5472
9. Kakita A, Goldman JE (1999) Patterns and dynamics of SVZ cell migration in the postnatal forebrain: monitoring living progenitors in slice preparations. Neuron 23:461–472. doi:S0896-6273(00)80800-4
10. Gensert JM, Goldman JE (2001) Heterogeneity of cycling glial progenitors in the adult mammalian cortex and white matter. J Neurobiol 48:75–86. doi:10.1002/neu.1043
11. Mason JL, Goldman JE (2002) A2B5+ and O4+ cycling progenitors in the adult forebrain white matter respond differentially to PDGF-AA, FGF-2, and IGF-1. Mol Cell Neurosci 20:30–42. doi:10.1006/mcne.2002.1114
12. D'Amico R, Lei L, Kennedy BC, Sisti J, Ebiana V, Crisman C, Christensen JG, Gil O, Rosenfeld SS, Canoll P, Bruce JN (2012) The addition of Sunitinib to radiation delays tumor growth in a murine model of glioblastoma. Neurol Res 34:252–261. doi:10.1179/1743132812Y.0000000005
13. Gao X, McDonald JT, Hlatky L, Enderling H (2013) Acute and fractionated irradiation differentially modulate glioma stem cell division kinetics. Cancer Res. doi:10.1158/0008-5472
14. Hsieh CH, Wu CP, Lee HT, Liang JA, Yu CY, Lin YJ (2012) NADPH oxidase subunit 4 mediates cycling hypoxia-promoted radiation resistance in glioblastoma multiforme. Free Radic Biol Med 53:649–658. doi:10.1016/j.freeradbiomed.2012.06.009
15. Lee J, Kotliarova S, Kotliarov Y, Li A, Su Q, Donin NM, Pastorino S, Purow BW, Christopher N, Zhang W, Park JK, Fine HA (2006) Tumor stem cells derived from glioblastomas cultured in bFGF and EGF more closely mirror the phenotype and genotype of primary tumors than do serum-cultured cell lines. Cancer Cell 9:391–403. doi:10.1016/j.ccr.2006.03.030
16. Silber JR, Bobola MS, Blank A, Chamberlain MC (2012) O(6)-Methylguanine- DNA methyltransferase in glioma therapy: promise and problems. Biochim Biophys Acta 1826:71–82. doi:10.1016/j.bbcan.2011.12.004
17. Schulte A, Gunther HS, Phillips HS, Kemming D, Martens T, Kharbanda S, Soriano RH, Modrusan Z, Zapf S, Westphal M, Lamszus K (2011) A distinct subset of glioma cell lines with stem cell-like properties reflects the transcriptional phenotype of glioblastomas and overexpresses CXCR4 as therapeutic target. Glia 59:590–602. doi:10.1002/glia.21127
18. Sturm D, Witt H, Hovestadt V, Khuong-Quang DA, Jones DT, Konermann C, Pfaff E, Tonjes M, Sill M, Bender S, Kool M, Zapatka M, Becker N, Zucknick M, Hielscher T, Liu XY, Fontebasso AM, Ryzhova M, Albrecht S, Jacob K, Wolter M, Ebinger M, Schuhmann MU, van Meter T, Fruhwald MC, Hauch H, Pekrun A, Radlwimmer B, Niehues T, von Komorowski G, Durken M, Kulozik AE, Madden J, Donson A, Foreman NK, Drissi R, Fouladi M, Scheurlen W, von Deimling A, Monoranu C, Roggendorf W, Herold-Mende C, Unterberg A, Kramm CM, Felsberg J, Hartmann C, Wiestler B, Wick W, Milde T, Witt O, Lindroth AM, Schwartzentruber J, Faury D, Fleming A, Zakrzewska M, Liberski PP, Zakrzewski K, Hauser P, Garami M, Klekner A, Bognar L, Morrissy S, Cavalli F, Taylor MD, van Sluis P, Koster J, Versteeg R, Volckmann R, Mikkelsen T, Aldape K, Reifenberger G, Collins VP, Majewski J, Korshunov A, Lichter P, Plass C, Jabado N, Pfister SM (2012) Hotspot mutations in H3F3A and IDH1 define distinct epigenetic and biological subgroups of glioblastoma. Cancer Cell 22:425–437. doi:10.1016/j.ccr.2012.08.024
19. Noushmehr H, Weisenberger DJ, Diefes K, Phillips HS, Pujara K, Berman BP, Pan F, Pelloski CE, Sulman EP, Bhat KP, Verhaak RG, Hoadley KA, Hayes DN, Perou CM, Schmidt HK, Ding L, Wilson RK, Van Den Berg D, Shen H, Bengtsson H, Neuvial P, Cope LM, Buckley J, Herman JG, Baylin SB, Laird PW, Aldape K (2010) Identification of a CpG island methylator phenotype that defines a distinct subgroup of glioma. Cancer Cell 17:510–522. doi:10.1016/j.ccr.2010.03.017